*Physics – Uspekhi* **60** (9) 902 – 910 (2017) ©2017 Uspekhi Fizicheskikh Nauk, Russian Academy of Sciences

*REVIEWS OF TOPICAL PROBLEMS* PACS numbers: 72.20.Ht, 72.20.Jv, 72.80.Sk, 73.40.Sx

# Hot electrons in silicon oxide

V A Gritsenko

DOI: https://doi.org/10.3367/UFNe.2016.12.038008

## Contents


1. **Introduction** **902**
2. **Transport of electrons in $SiO_2$ in a weak electric field ($10^4$–$10^6$ V cm$^{-1}$)** **903**
3. **Methods of studying the distribution function of hot electrons over energy in $SiO_2$ in high electric fields** **904**
   3.1 Electroluminescence; 3.2 Determination of the average energy of electrons in $SiO_2$ by the separation of the electron and hole components of the current traversing a transistor; 3.3 Emission of electrons from $SiO_2$ into a vacuum
4. **Hole injection into $SiO_2$ caused by electron heating** **908**
5. **Electron heating in silicon oxynitride ($SiO_xN_y$) and nitride ($Si_3N_4$)** **908**
6. **Conclusion** **909**
   **References** **909**


**Abstract. One particular application of amorphous silicon oxide ($SiO_2$), a material crucial for silicon device technology and design, is as a flash memory tunnel dielectric. The breakdown field of $SiO_2$ exceeds $10^7$ V cm$^{-1}$. Strong electric fields in $SiO_2$ give rise to phenomena that do not occur in crystalline semiconductors. In relatively weak electric fields ($10^4 - 10^6$ V cm$^{-1}$), the electron distribution function is determined by the scattering of electrons on longitudinal optical phonons. In high fields (in excess of $10^6$ V cm$^{-1}$), the distribution function is determined by electron–acoustic phonon scattering.**

**Keywords:** silicon oxide, hot electrons, scattering, optical phonons

## 1. Introduction

In the crystalline semiconductors, because of the small bandgap energy and high mobility of electrons and holes, an avalanche breakdown is observed in the electric fields ranging $10^4 - 10^5$ V cm$^{-1}$. The breakdown fields of thermal $SiO_2$ on silicon are more than $10^7$ V cm$^{-1}$. In such fields, new uncommon effects show themselves. The high electric fields ($\approx 10^7$ V cm$^{-1}$) in $SiO_2$ are realized in flash-memory devices. At present, being produced on the mass market, flash memory based on the floating gate prevails. In such memory elements, the floating polysilicon gate is separated from the silicon substrate by an $SiO_2$ layer 5–10 nm thick [1]. The reprogramming of such a memory element is achieved in an electric field of $\approx 10^7$ V cm$^{-1}$ via the injection of electrons and holes from silicon into the polysilicon gate. If we assume that the electrons in $SiO_2$ are not scattered at a length equal to the maximum thickness of the oxide, $d = 10$ nm, then the electrons can gain an energy $E = Fd = 10^7 \times 10^{-6} = 10$ eV ($F$ is the electric field strength). Certainly, the assumption that the electrons in $SiO_2$ are not scattered is unreal. Nevertheless, it follows from the experiments presented in this survey that in a high electric field the electrons in $SiO_2$ can gain an energy of up to several electron-volts, up to 10 eV [2].

Under the conditions of an enhanced radiation background, an energy-independent memory based on silicon–oxide–nitride–oxide–silicon (SONOS) structures is used [1, 3–7]. In SONOS structures, it is the amorphous silicon nitride ($Si_3N_4$) that takes the part of a memory medium. Silicon nitride has a high concentration of deep ($\approx 1.5$ eV) traps capable of localizing electrons and holes [8, 9]. The lifetime of electrons and holes localized in silicon nitride reaches 10 years at 85 °C [1]. This time corresponds to the time of information storage in flash-memory devices. The reprogramming of SONOS devices is implemented through a tunnel oxide 1.8–5.0 nm thick [1, 3, 5]. To overcome the problem of mutual influence of the adjacent floating gates in memory matrices with floating gates, elements of a flash-memory are currently being developed in which silicon nitride appears in the role of a memory medium and a dielectric with a high dielectric constant (so-called high-$k$ dielectric) is employed as the blocking layer, instead of $SiO_2$ [1, 10, 11]. One of the variants of such a memory element comprises a $TaN - Al_2O_3 - Si_3N_4 - SiO_2 - Si$ (TANOS) structure [5, 12].

At present, the concept of a vertical three-dimensional memory is being framed for increasing the flash-memory storage capacity [13]. Prototypes of such a memory have been developed, in which 32 layers are used. Silicon nitride takes the role of a memory medium in three-dimensional memory; as the tunnel oxide, $SiO_2$ with a thickness of 3.5 nm is employed. The reprogramming is implemented via the

**V A Gritsenko** Rzhanov Institute of Semiconductor Physics, Siberian Branch of the Russian Academy of Sciences,
prosp. Lavrent'eva 13, 630090 Novosibirsk, Russian Federation;
Novosibirsk State University,
ul. Pirogova 2, 630090 Novosibirsk, Russian Federation;
Novosibirsk State Technical University,
prosp. K. Marksa 20, 630073 Novosibirsk, Russian Federation
E-mail: grits@isp.nsc.ru

Received 2 September 2016, revised 7 December 2016
*Uspekhi Fizicheskikh Nauk* **187** (9) 971 – 979 (2017)
DOI: https://doi.org/10.3367/UFNr.2016.12.038008
Translated by S N Gorin; edited by A Radzig

alternating injection and subsequent localization of electrons and holes in the silicon nitride. The electric field in the tunnel oxide of such a memory element reaches $\approx 10^7$ V cm$^{-1}$.

Electron heating in a high electric field on the order of $10^7$ V cm$^{-1}$ can lead to the formation of defects, subsequent trapping of electrons and holes, and degradation of the electrical properties of $SiO_2$ [14, 15]. In silicon devices, amorphous $SiO_2$ is widely exploited. The bandgap energy of amorphous $SiO_2$ amounts to 8.0 eV [16]. The energies of longitudinal optical phonons in $SiO_2$ are equal to 0.153 and 0.063 eV. In this paper, we analyze the phenomena of electron heating in a high electric field in silicon oxide, and also in dielectrics with a high density of traps: silicon nitride and silicon oxynitride.

## 2. Transport of electrons in $SiO_2$ in a weak electric field ($10^4 - 10^6$ V cm$^{-1}$)

Direct measurements of the mobility of nonequilibrium electrons in fused quartz were carried out in Refs [17, 18]. The nonequilibrium electrons were generated with the aid of X-rays. The transit time of the packet of electrons was measured. In the range of the electric field strengths of $3\times10^3 - 1\times10^5$ V cm$^{-1}$, the drift velocity of electrons is proportional to the field strength. Figure 1 depicts the dependence of the electron mobility on the reciprocal temperature in amorphous $SiO_2$. The straight line corresponds to the Thornber–Feynman model [19] for scattering on longitudinal optical (LO) phonons. In amorphous $SiO_2$, the electron mobility is $\mu = 20 \pm 3$ cm$^2$ V$^{-1}$ s$^{-1}$ at 298 K. The effective mass of the free electron equals $m^* = 1.4 m_0$. At a temperature below 200 K, the mobility ceases to depend on temperature; its value is about 40 cm$^2$ V$^{-1}$ s$^{-1}$.

Simulating electron transport by the Monte Carlo method in relatively weak electric fields ($10^4 - 1\times10^6$ V cm$^{-1}$) was carried out in Refs [20–22]. The electron scattering in $SiO_2$ on longitudinal optical phonons with an energy of 0.15 and 0.06 eV was taken into account. Figure 2 plots the trajectories of injected electrons in different electric fields. For a field of $10^4$ V cm$^{-1}$, the electron trajectory shows a diffuse character: an increase in the field strength leads to the orientation of scattering along the electric field [22].

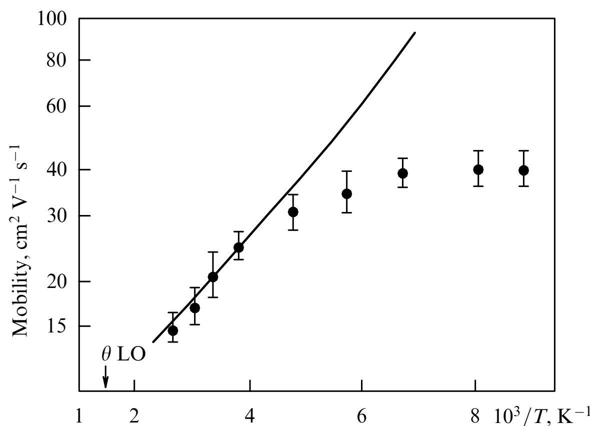


**Figure 1.** Temperature dependence of the drift mobility of electrons in amorphous $SiO_2$. The straight line corresponds to the Thornber–Feynman theory [19] of electron scattering on longitudinal optical (LO) phonons. The arrow indicates the Debye temperature.

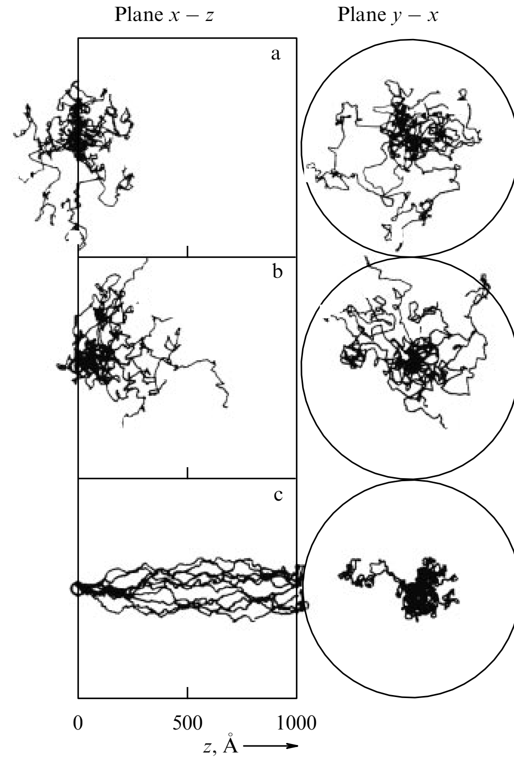


**Figure 2.** Trajectory of an electron (injected with an initial energy of 0.1 eV) along a field (a) $F = 10^4$ V cm$^{-1}$, (b) $10^5$ V cm$^{-1}$, and (c) $10^6$ V cm$^{-1}$ [21].

In the fields of $(0.3–2.8)\times10^6$ V cm$^{-1}$, electron scattering on the longitudinal optical phonons prevails (Fig. 3) [22]. The mean free path of electrons in $SiO_2$ was determined in electric fields of $10^5 - 2\times10^6$ V cm$^{-1}$ in experiments on the scattering of photoinjected electrons from a metal [23] in a metal–oxide–semiconductor (MOS) structure. The expression for the electron potential in the dielectric at a distance $x$ from the metal takes the form

$$\Phi(x) = \Phi_0 + \int_0^x F(z)\,\mathrm{d}z - \frac{q}{16\pi\varepsilon x}\,. \tag{1}$$

Figure 4 depicts the electron potential in a dielectric near the boundary with the metal [23].

In paper [23], it was shown that the dependence of the probability of electron injection upon excitation by a light quantum $\hbar\omega$ in an electric field $F$ is given by the expression

$$J = A(\hbar\omega)(\hbar\omega - \Phi + \beta\sqrt{F})^k \exp\left(-\frac{X_\mathrm{m}}{L}\right),$$
$$X_\mathrm{m} = \frac{1}{2\sqrt{F}}\,, \qquad \beta = \sqrt{\frac{q^3}{4\pi\varepsilon\varepsilon_0}}\,. \tag{2}$$

Here, $A(\hbar\omega)$ is the instrument function, which reflects the dependence of the number of quanta on the energy of the quanta; $\beta$ is the Schottky constant; $\varepsilon$ is the optical dielectric constant; $k$ is a parameter whose value depends on the mechanism of electron scattering in the emitter, and $X_\mathrm{m}$ is the distance from the metal–dielectric interface to the potential maximum. Figure 5 illustrates the dependence of the photoemission current on the field strength in silicon oxide [23]. A good agreement of the results of the experiments and calculations is observed at the mean free path $L = 3.4$ nm. Similar experiments regarding the mean free path of electrons

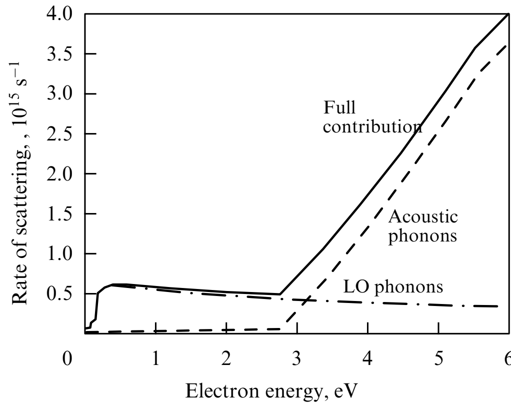


**Figure 3.** Rate of electron scattering depending on the energy of electrons for different mechanisms of scattering at 298 K.

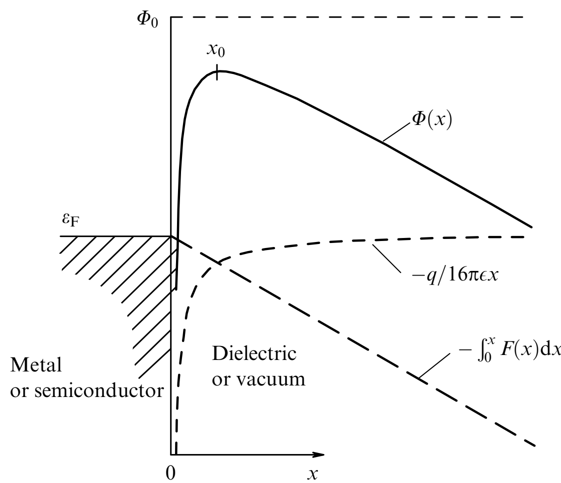


**Figure 4.** Potential of an electron in the dielectric near the boundary with a metal. The dashed lines correspond to the potential of the image forces and to the potential corresponding to the applied field. The solid line depicts the total potential of an electron. The processes of phonon emission and absorption are taken into account.

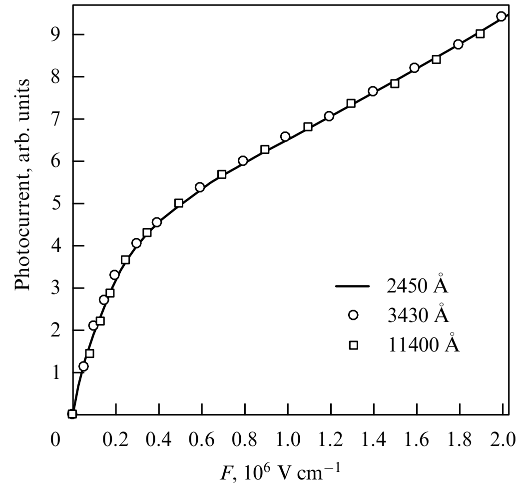


**Figure 5.** Dependence of the photoemission current on the electric field strength upon the photoemission of electrons from silicon into $SiO_2$; the thickness of the $SiO_2$ layer is 245 nm [22].

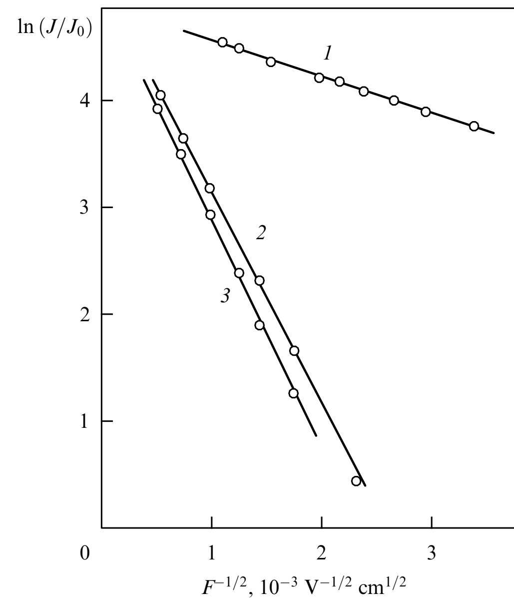


**Figure 6.** Dependence of the photoemission current of electrons on the electric field in $SiO_2$ (curve *1*) for the quantum energy of 5.0 eV, and in $SiO_xN_y$ for the quantum energy of 5.0 eV (curve *2*) and 4.5 eV (curve *3*) [24].

in $SiO_2$ and in silicon oxynitride ($SiO_xN_y$) with a composition close to $SiO_2$ were performed in paper [24].

Figure 6 presents the dependence of the photoemission current of electrons on the electric field in the coordinates corresponding to expression (2). The mean free path of electrons in $SiO_2$, retrieved from Fig. 6, equals 3.5 nm. The mean free path of electrons in $SiO_xN_y$ is 0.5 nm. Notice that the length of the Si–O bond in $SiO_2$ is equal to 0.162 nm [25]. A simulation by the Monte Carlo method indicates that electron scattering on longitudinal optical phonons does not stabilize the distribution function of electrons in $SiO_2$ in an electric field with a strength exceeding $2 \times 10^6$ V cm$^{-1}$ [26].

## 3. Methods of studying the distribution function of hot electrons over energy in $SiO_2$ in high electric fields

### 3.1 Electroluminescence

Experiments were performed on metal–dielectric–semiconductor structures (Fig. 7a) [22, 25, 27, 28]. Silicon suboxide ($SiO_x$) enriched in silicon was used to inject electrons into $SiO_2$. The data obtained from measurements by the method of photoelectron spectroscopy show that, in the first approximation, $SiO_x$ comprises a mixture of two phases: Si (silicon islets with a size of $\sim$ 5 nm) and $SiO_2$ [29]. Figure 7b presents schematically the Si–$SiO_x$–$SiO_2$–Al structure that was used in the experiment on electroluminescence [28]. In this experiment, electrons from degenerate $n^+$ type silicon are injected into $SiO_x$. In silicon suboxide, tunneling of electrons between Si islets and then their tunneling from silicon islets into $SiO_2$ proceeds. The injection of electrons from $SiO_x$ into $SiO_2$ can occur in a relatively weak electric field, since a local strengthening of the electric field takes place near the silicon islets. Hot electrons in $SiO_2$ lose energy on surface plasmons in the anode (aluminum). A more efficient interaction is observed on the rough surface of the anode [27, 28]. Quantum yield of luminescence in the interaction of hot electrons with the surface plasmons amounts to $\sim 10^{-6}$ electrons per photon [27].

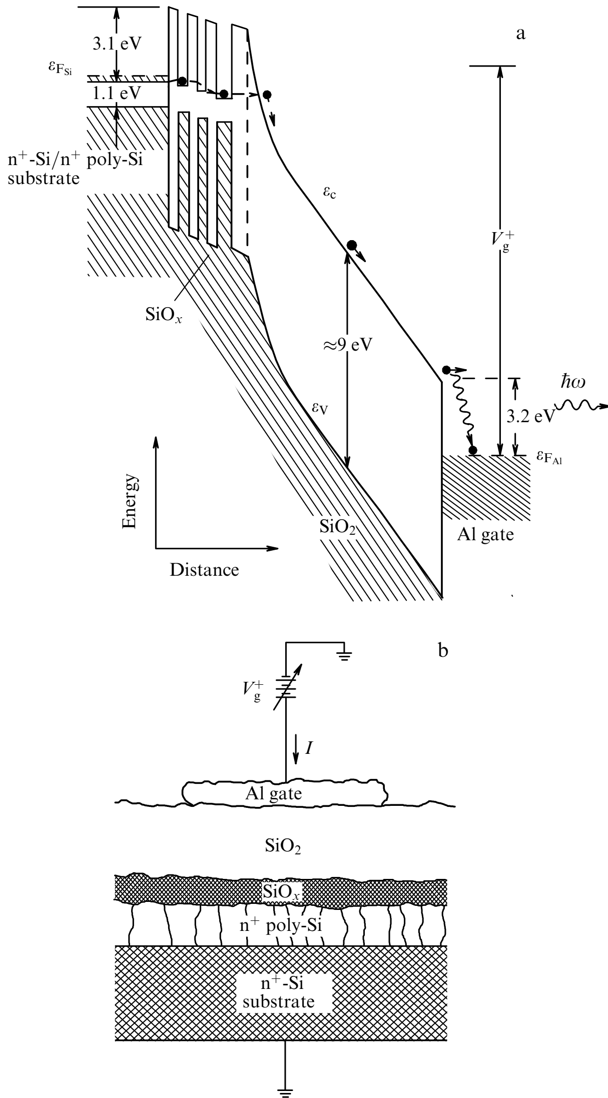


**Figure 7.** (a) Energy diagram and (b) schematic structure of the device, which illustrate the electroluminescence experiment on determining the distribution function of hot electrons in $SiO_2$ [22]. The electrons are injected from the silicon substrate into the injector–silicon oxide enriched in silicon ($SiO_x$) to prevent the breakdown of $SiO_2$. Some of the electrons injected from $SiO_2$ lose their energy in the metallic gate, emitting surface plasmons at the metal–vacuum boundary. The plasmons are decomposed with the emission of a light quantum. The average energy of electrons is retrieved from the spectrum of the emitted photons.

Figure 8 depicts the dependence of the number of photons on the energy in the Si–$SiO_x$–$SiO_2$–Al structure in the case of a positive potential at aluminum for three values of the electric field strength in $SiO_2$ at the $SiO_2$–Al boundary [27]. The optical system is restricted by the photon energy of 5 eV. The barrier height for the electrons at the Al–$SiO_2$ boundary is equal to 3.2 eV [30]. A detailed quantitative model of an electron–plasmon interaction for hot electrons in aluminum is nonexistent; however, some assumptions can be made. If the energy of electrons in $SiO_2$ relative to the bottom of the conduction band is small, the luminescence spectrum should fall sharply at an energy exceeding 3.2 eV. Figure 8 gives evidence that the electrons in $SiO_2$ are heated substantially; the average energy of electrons considerably exceeds the energy $E_c$ at the edge of the conduction band in $SiO_2$.

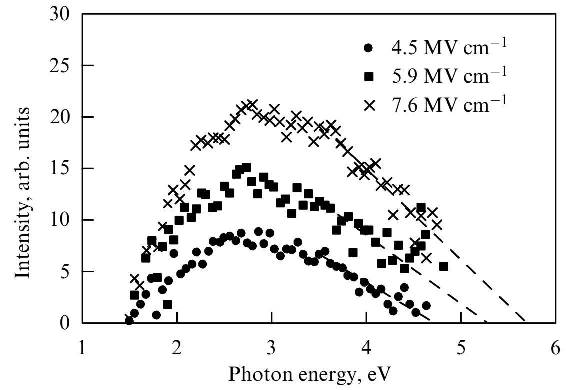


**Figure 8.** Dependence of the number of photons on the energy of photons in the Si–$SiO_x$–$SiO_2$–Al structure at a positive potential at aluminum for three values of the electric field strength in $SiO_2$ at the $SiO_2$–Al boundary [27].

### 3.2 Determination of the average energy of electrons in $SiO_2$ by the separation of the electron and hole components of the current traversing a transistor

The method of separating the electron and hole components of the current flowing in a dielectric was first proposed for determining the sign of charge carriers in silicon nitride ($Si_3N_4$) [31]. A similar method was applied in Refs [26, 28] for studying hot electrons in $SiO_2$. Figure 9 shows an energy diagram and the scheme of the inclusion of a field-effect p-channel transistor in an experiment on the separation of the electron and hole components of current in $SiO_2$ [26]. To increase the efficiency of the injection of electrons into $SiO_2$, the silicon suboxide ($SiO_x$) was utilized as the cathode. The method of separating electrons and holes in a dielectric is discussed in detail in paper [32]. The current of electrons injected from $SiO_x$ into $SiO_2$ is registered in the substrate circuit (Fig. 9b). The current of holes injected from the silicon substrate into $SiO_2$ is recorded in the circuit involving channel. The average energy necessary for the generation of an electron–hole pair in silicon is equal to 4.3 eV [33, 34]. The procedure for retrieving the average energy of electrons from the dependence on the electric field is described in Refs [27, 29]. Figure 10 presents the dependence of the average electron energy in $SiO_2$ on the electric field [32]. From the slope of this dependence, the electron mean free path can be determined as being $L \approx 2.3$ nm. It follows from Fig. 10 that in a strong electric field the electron energy in $SiO_2$ can reach 7–9 eV.

### 3.3 Emission of electrons from $SiO_2$ into a vacuum

The experiment is based on the determination of the energy distribution of electrons injected from $SiO_2$ into a vacuum through a thin metal layer applying the retarding potential method. Figure 11 plots an energy diagram, which illustrates the measurement of the distribution function of hot electrons injected from $SiO_2$ through aluminum into a vacuum (Fig. 11a), and the schematic structure of the capacitor used for the experiment (Fig. 11b) [22]. The experiment was carried out using an Si–$SiO_x$–$SiO_2$–metal structure. As the metal, Al, Cr, or Au 15–20 nm thick was used. The injection of electrons into $SiO_2$ is implemented from $SiO_x$.

Figure 12 presents the dependence of the current of electron emission into a vacuum on the value of the retarding potential [32]. The energy distribution of electrons for three values of the electric field strength and also the data of

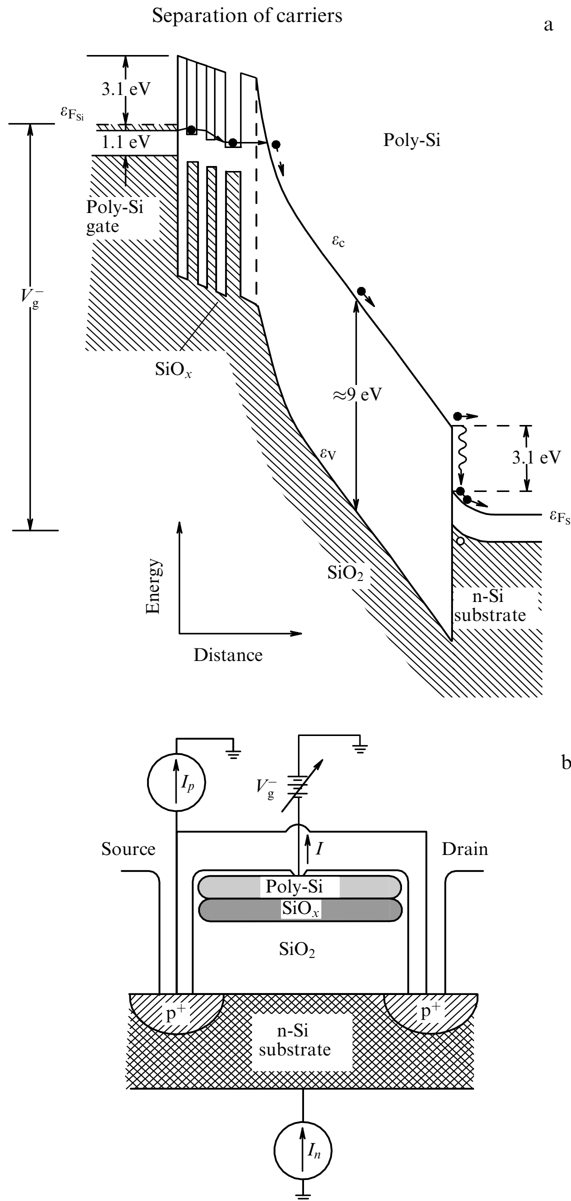


**Figure 9.** (a) Energy diagram and (b) schematic structure of the device, which illustrate the experiment on the separation of electrons and holes in $SiO_2$ [28]. The electrons are injected from the polysilicon gate of a field-effect transistor through $SiO_x$ and $SiO_2$ into the silicon substrate. The number of electron–hole pairs entering into the substrate, which are generated by hot electrons, is registered in the circuit with the source and/or drain. The electron current is registered in the substrate circuit. The average energy of carriers is determined using the known ionization probability in silicon as a function of the electron energy.

theoretical calculations are given in Fig. 13 [22]. The calculated curves were obtained by the Monte Carlo method without and taking into account collisional broadening effects. The maximum of the distribution function of hot electrons lies at an energy of approximately 3 eV. From the dependence of the average energy of hot electrons on the electric field strength, the mean free path of electrons was estimated to be $L \approx 3.2$ nm [32]. It was also reported in [32] that in an $SiO_2$ layer with a thickness of 150 nm in an average electric field of $5 \times 10^6$ V cm$^{-1}$ the energy of hot electrons in $SiO_2$ can reach 40 eV.

A drawback of the above experiments lies in the uncertainty caused by electron scattering in the metal

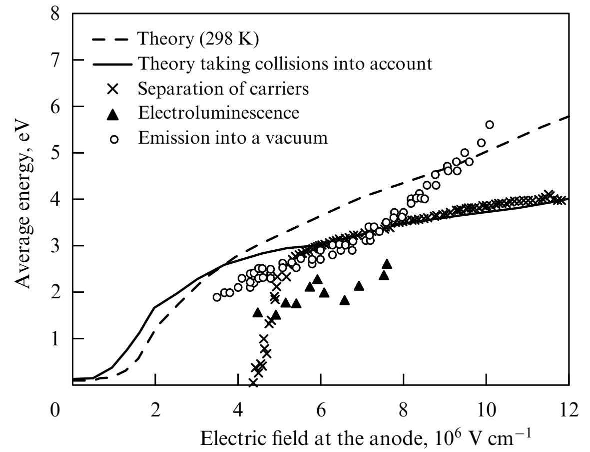


**Figure 10.** Distribution function (average energy of hot electrons) depending on the strength of the average electric field according to the data of three experiments: on the separation of the electron and hole components of current; electroluminescence, and emission of electrons into a vacuum. In experiments on the electroluminescence and emission into a vacuum, the average energy was measured relative to the Fermi level in aluminum; in the experiment on the separation of the electron and hole components of current, the electron energy was measured relative to the bottom of the conduction band in silicon. The dashed line indicates the position of the bottom of the conduction band in $SiO_2$.

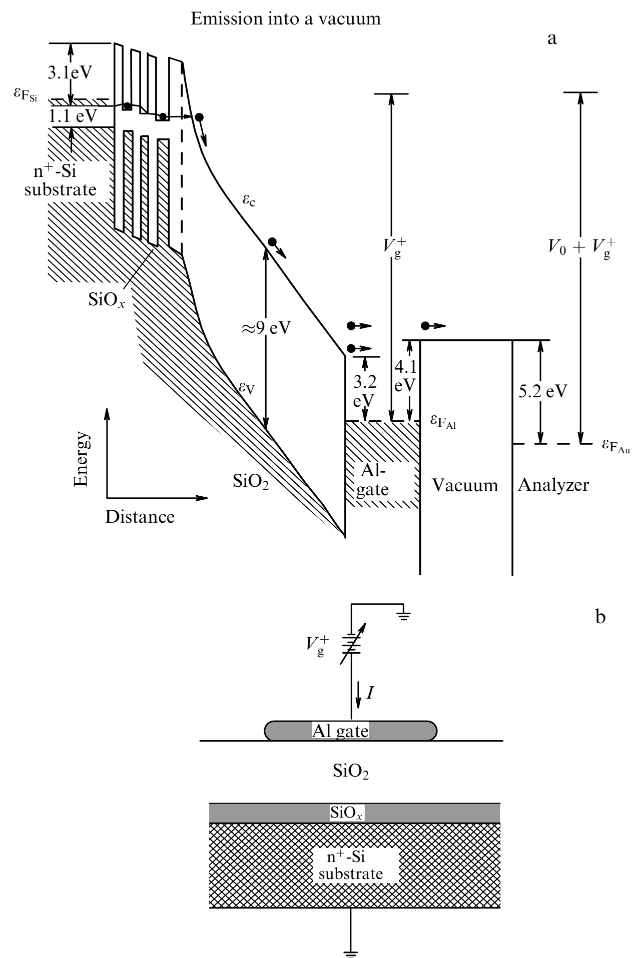


**Figure 11.** (a) Energy diagram and (b) schematic structure of the device in the experiment for the determination of the distribution function of electrons upon emission into a vacuum. The injected electrons pass through a thin (≈ 25 nm) metal gate into a vacuum. The energy distribution of electrons is measured in the vacuum chamber by the retarding potential method.

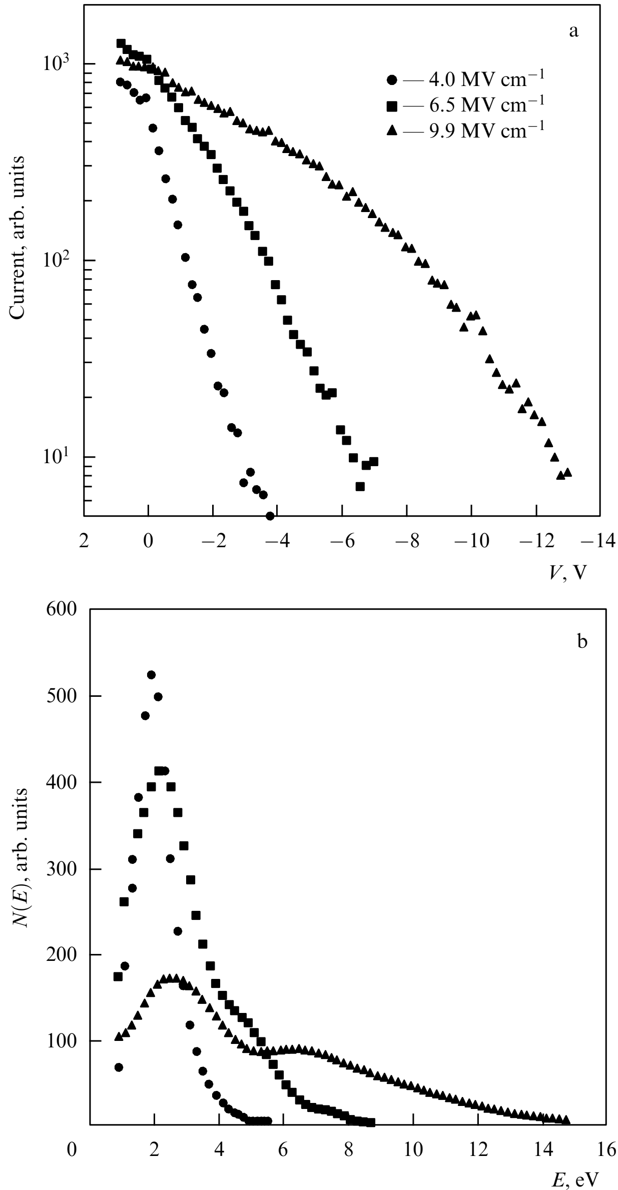


**Figure 12.** (a) Current of electrons emitted from $SiO_2$ into a vacuum depending on the retarding potential for three values of the electric field strength. (b) Distribution function of electrons obtained by the differentiation of the data presented in figure (a). The thickness of the $SiO_2$ layer is 50 nm; the thickness of the A1 layer is 25 nm.

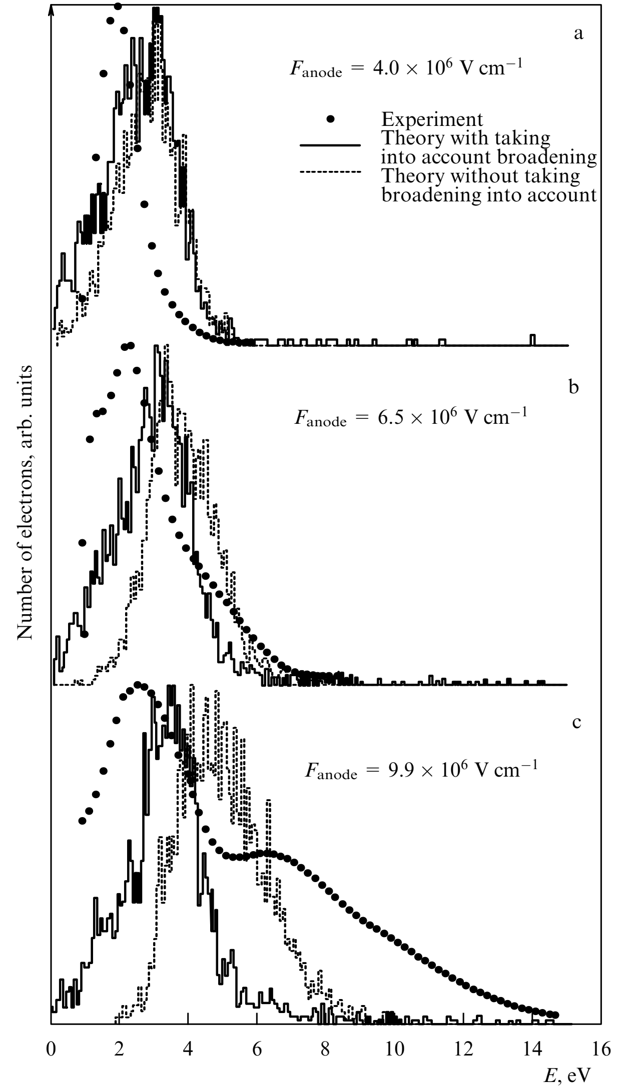


**Figure 13.** Distribution function of hot electrons in an $SiO_2$ layer 50 nm thick, obtained from the experiments on the emission of electrons into a vacuum through a metal, and its comparison with the calculated distribution function obtained by the Monte Carlo method taking into account the broadening due to collisions and without collisions.

through which the emission of electrons into a vacuum is implemented. It was established in paper [32] that the distribution function of hot electrons in $SiO_2$ depends substantially on the type of metal (Al, Cr, Au). The procedure for determining the distribution function of hot electrons emitted directly from $SiO_2$ into a vacuum has no such drawback [35, 36]. In this procedure, an Si–$SiO_2$ structure was utilized; a positive charge (positively charged ions) from the plasma of a corona discharge in the atmosphere was deposited onto the $SiO_2$ surface. After this, the surface of the sample is irradiated by the light source with an energy that exceeds the barrier for the photoemission of electrons from Si into $SiO_2$. The photoinjected electrons are accelerated in $SiO_2$ and are emitted into a vacuum. The energy distribution of the electrons injected into a vacuum is measured by the retarding potential method. This method makes it possible to study the distribution function of electrons injected in relatively weak electric fields (2–4) $\times 10^6$ V cm$^{-1}$.

Figure 14 depicts the distribution function of hot electrons emitted from a thermal $SiO_2$ layer with a thickness of 63 nm into a vacuum at different values of the electric field [36]. An increase in the electric field strength in the dielectric from $0.8 \times 10^6$ to $5 \times 10^6$ V cm$^{-1}$ is accompanied by a shift of the maximum in the distribution function of electrons from 0.5 to 2.5 eV.

An increase in the thickness of the silicon oxide layer from 2.8 to 76 nm at close values of the electric field strength leads to a shift of the distribution function maximum from 1 to 3 eV (Fig. 15) [36]. An analysis has shown that the presence of metal only insignificantly distorts the distribution function of the electrons in the vacuum. It follows from Fig. 15 that the distribution function of hot electrons emitted into a vacuum depends on the thickness of $SiO_2$ layer. The distribution function is shifted in the direction of higher energies with an increase in the thickness of the silicon oxide layer. This result indicates the dependence of the distribution function of hot electrons on the coordinate.

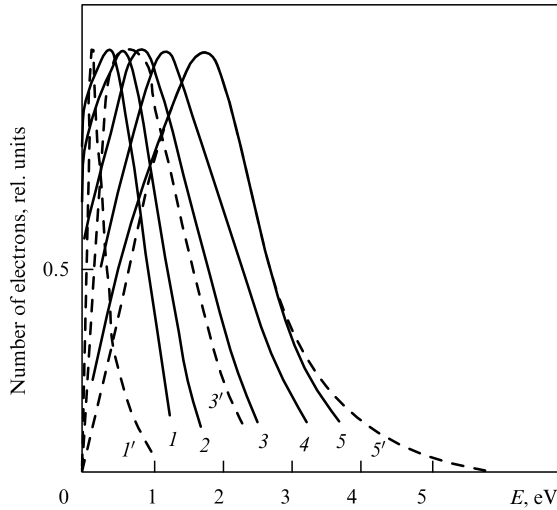


**Figure 14.** Distribution function of electrons emitted from an $SiO_2$ layer 63 nm thick in different electric fields: (*1*) $F = 0.8 \times 10^6$ V cm$^{-1}$, (*2*) $1.1 \times 10^6$ V cm$^{-1}$, (*3*) $1.6 \times 10^6$ V cm$^{-1}$, (*4*) $3.1 \times 10^6$ V cm$^{-1}$, and (*5*) $5.6 \times 10^6$ V cm$^{-1}$. Curves *1'*, *3'*, and *5'* are calculated.

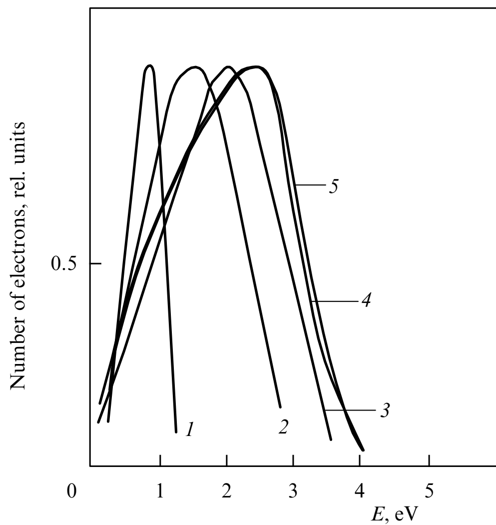


**Figure 15.** Distribution function of electrons emitted from $SiO_2$ layers of different thicknesses $d$ into a vacuum: (*1*) $d = 2.8$ nm, $F = 5.5 \times 10^6$ V cm$^{-1}$; (*2*) $d = 6.8$ nm, $F = 5.3 \times 10^6$ V cm$^{-1}$; (*3*) $d = 32.3$ nm, $F = 5.6 \times 10^6$ V cm$^{-1}$; (*4*), $d = 63$ nm, $F = 5.6 \times 10^6$ V cm$^{-1}$, and (*5*) $d = 76$ nm, $F = 5.4 \times 10^6$ V cm$^{-1}$.

In Refs [37, 38], the Monte Carlo method was applied to calculating the distribution function of electrons in $SiO_2$ in the regime of ballistic transfer upon their scattering on longitudinal optical phonons with energies of 0.063 and 0.153 eV. The results of the calculations were compared with the distribution function of the electrons emitted into a vacuum. The peaks caused by electron scattering on low- and high-energy longitudinal optical phonons were observed in the distribution function.

## 4. Hole injection into $SiO_2$ caused by electron heating

The heating of electrons injected from silicon into silicon oxide is accompanied by hole injection from the polysilicon contact into silicon oxide [14]. It is assumed that the hot

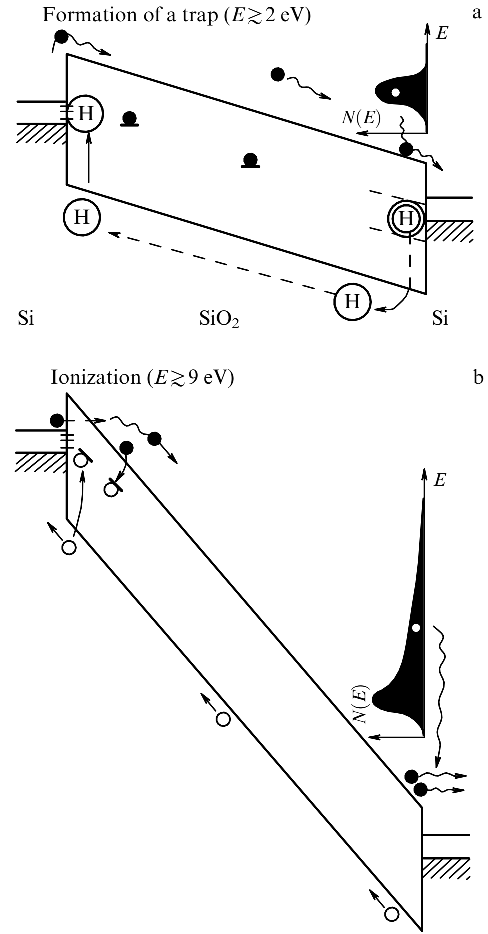


**Figure 16.** (a) Energy diagram of a silicon–silicon oxide–polysilicon structure with a positive potential at polysilicon in a weak electric field. (b) Electrons injected from silicon become heated in the silicon-oxide layer and generate holes (H) in the polysilicon layer, which are injected into the silicon oxide.

electrons injected from the silicon oxide into polysilicon generate hot holes in the polysilicon (Fig. 16a). The energy of the holes exceeds the height of the hole barrier at the polysilicon–silicon oxide boundary; therefore, holes from the polysilicon are injected into the silicon oxide (Fig. 16b) [14]. Hole traps exist near the boundary between the silicon and thermal silicon oxide. The holes injected into the silicon oxide can be captured by these hole traps (Fig. 17) [15].

## 5. Electron heating in silicon oxynitride ($SiO_xN_y$) and nitride ($Si_3N_4$)

Silicon oxynitride ($SiO_xN_y$) is utilized as a subgate dielectric in logical low-power silicon devices [7]. The energy gap width of the $SiO_xN_y$, depending on the chemical composition, changes in the range of 4.5–8.0 eV [39, 40]. The amorphous silicon nitride ($Si_3N_4$) has an energy gap width equal to 4.5 eV [41]. Silicon nitride possesses a high number density ($\sim 10^{19}$ cm$^{-3}$) of electron and hole traps with an energy of 1.4 eV [42, 43]. The localization of electrons and holes in silicon nitride is employed for the accumulation of charges in flash-memory devices [1, 7]. The electron heating in silicon nitride and silicon oxynitride was studied in Refs [36, 42]. The emission of electrons from the dielectric into a vacuum has been investigated. The silicon suboxide $SiO_x$ enriched in

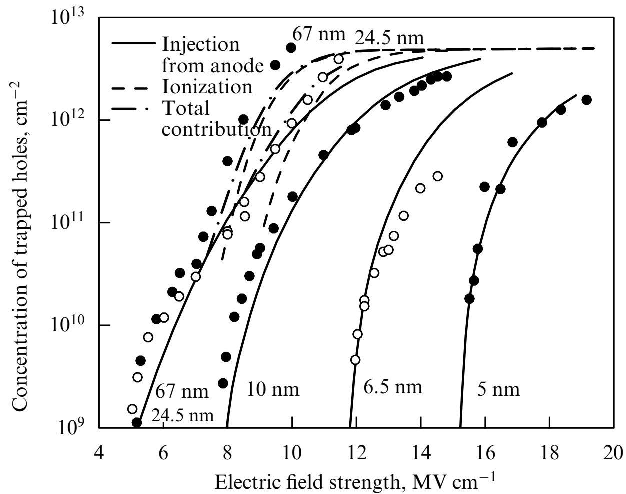


**Figure 17.** Surface density of a positive charge depending on the field strength at different thicknesses of the silicon-oxide layer.

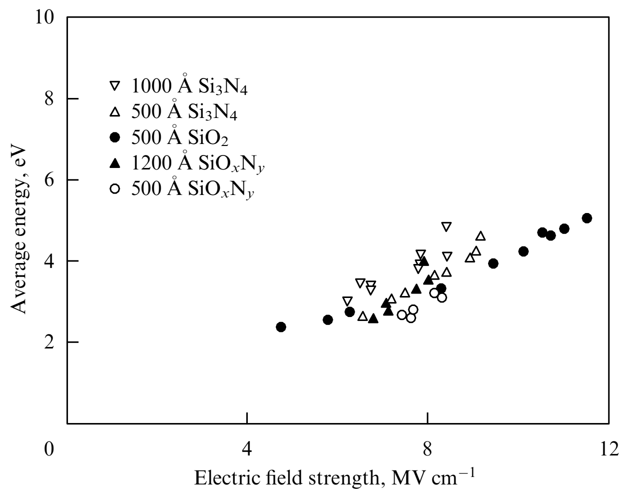


**Figure 18.** Average energy of electrons in the silicon oxide, silicon nitride, and silicon oxynitride layers of different thicknesses depending on the electric field strength. The electron energy is counted from the bottom of the conduction band in the dielectric.

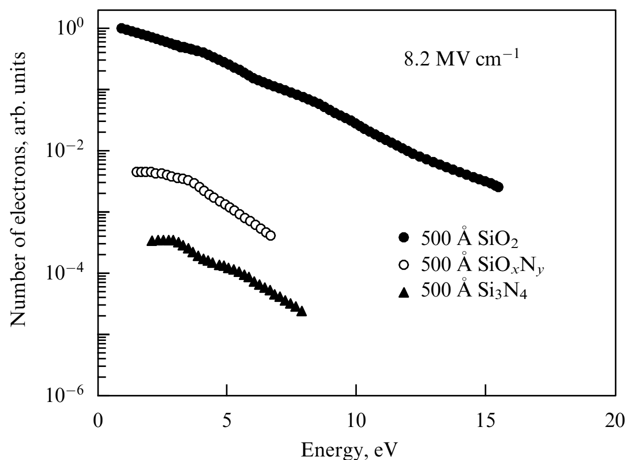


**Figure 19.** Electron-energy distribution for silicon oxide, silicon nitride, and silicon oxynitride in an electric field of $8.2 \times 10^6$ V cm$^{-1}$.

silicon took the part of the injector of electrons into the silicon nitride and oxynitride.

The dependence of the energy of electrons in $SiO_2$, $SiO_xN_y$, and $Si_3N_4$ on the electric field strength is presented in Fig. 18 [44]. It can be seen that the energy distributions of electrons for these materials are similar to each other. Figure 19 presents the relative efficiency of emission from $SiO_2$, $SiO_xN_y$, and $Si_3N_4$ into a vacuum, depending on the energy of electrons [44]. The efficiency of emission from $SiO_xN_y$ is two orders of magnitude less, and from $Si_3N_4$ four orders of magnitude less, than that from $SiO_2$. The low efficiency of the emission of electrons from $SiO_xN_y$ and $Si_3N_4$ is caused by capturing electrons into the traps.

## 6. Conclusion

In relatively weak electric fields ($10^4$–$1 \times 10^6$ V cm$^{-1}$), the distribution function of electrons in $SiO_2$ is determined by their scattering on longitudinal optical phonons. In strong fields (> $10^6$ V cm$^{-1}$), the distribution function is determined by electron scattering on acoustic phonons. The heating of electrons injected from silicon into silicon oxide leads to the generation of hot holes in the polysilicon electrode and to their subsequent injection into the silicon oxide. Because of the localization of electrons it traps located in silicon nitride and in silicon oxynitride, the efficiency of the electron emission from $SiO_xN_y$ and $Si_3N_4$ is orders of magnitude less than that from $SiO_2$.

**Acknowledgments**

This study was partially supported by the Russian Scientific Foundation, grant No. 14-19-00192.

## References

1. Gritsenko V A "Flash pribory pamyati" ("Flash-memory devices"), in *Dielektriki v Nanoelektronike* (Dielectrics in Nanoelectronics) (Ed. A L Aseev) (Novosibirsk: Izd. SO RAN, 2010)
2. Fischetti M V, DiMaria D J *Phys. Rev. Lett.* **55** 2475 (1985)
3. Roizin Y, Gritsenko V, in *Dielectric Films for Advanced Microelectronics* (Eds M R Baklanov, M L Green, K Maex) (Chichester: John Wiley and Sons, 2007) p. 251
4. Wrazien S J et al. *Solid-State Electron.* **47** 885 (2003)
5. Lee C-H et al. *Appl. Phys. Lett.* **86** 152908 (2005)
6. Lisiansky M et al. *Appl. Phys. Lett.* **89** 153506 (2006)
7. Perevalov T V, Gritsenko V A *Phys. Usp.* **53** 561 (2010); *Usp. Fiz. Nauk* **180** 587 (2010)
8. Nasyrov K A, Shaimeev S S, Gritsenko V A, Han J H *J. Appl. Phys.* **105** 123709 (2009)
9. Vishnyakov A V, Novikov Yu N, Gritsenko V A, Nasyrov K A *Solid-State Electron.* **53** 25 (2009)
10. Gritsenko V A, Nasyrov K A "Transport and defects in advanced gate dielectrics", in *Nano and Giga Challenges in Microelectronics, Conf., September 10, Moscow, Russia, 2002*, p. 131
11. Gritsenko V A et al. *Solid-State Electron.* **47** 1651 (2003)
12. Lee C-H, Park K-C, Kim K *Appl. Phys. Lett.* **87** 073510 (2005)
13. Prince B *Vertical 3D Memory Technologies* (Chichester: John Wiley and Sons, 2014)
14. Fischetti M V *Phys. Rev. B* **31** 2099 (1985)
15. DiMaria D J, Cartier E, Buchanan D A *J. Appl. Phys.* **80** 304 (1996)
16. Nekrashevich S S, Gritsenko V A *Phys. Solid State* **56** 207 (2014); *Fiz. Tverd. Tela* **56** 209 (2014)
17. Hughes R C *Phys. Rev. Lett.* **30** 1333 (1973)
18. Hughes R C *Phys. Rev. Lett.* **35** 449 (1975)
19. Thornber K K, Feynman R P *Phys. Rev. B* **1** 4099 (1970)
20. Fitting H-J, Friemann J-U *Phys. Status Solidi A* **69** 349 (1982)
21. Fitting H-J, Boyde J *Phys. Status Solidi A* **75** 137 (1983)
22. Fischetti M V et al. *Phys. Rev. B* **31** 8124 (1985)

23. Berglund C N, Powell R J *J. Appl. Phys.* **42** 573 (1971)
24. Gritsenko V A, Mogil'nikov K P, Rzhanov A V *JETP Lett.* **27** 375 (1978); *Pis'ma Zh. Eksp. Teor Fiz.* **27** 400 (1978)
25. Gritsenko V A *Phys. Usp.* **51** 699 (2008); *Usp. Fiz. Nauk* **178** 727 (2008)
26. Theis T N et al. *Phys. Rev. Lett.* **52** 1445 (1984)
27. Theis T N et al. *Phys. Rev Lett.* **50** 750 (1983)
28. DiMaria D J et al. *J. Appl. Phys.* **57** 1214 (1985)
29. Novikov Yu N, Gritsenko V A *J. Appl. Phys.* **110** 014107 (2011)
30. Gritsenko V A *Stroenie i Elektronnaya Struktura Amorfnykh Dielektrikov v Kremnievykh MDP Strukturakh* (Atomic and Electronic Structure of Amorphous Dielectrics in Silicon MIS Structures) (Novosibirsk: Nauka, 1993)
31. Ginovker A S, Gritsenko V A, Sinitsa S P *Phys. Status Solidi B* **26** 489 (1974)
32. Brorson S D et al. *J. Appl. Phys.* **58** 1302 (1985)
33. Alig R C, Bloom S, Struck˚ W *Phys. Rev. B* **22** 5565 (1980)
34. Geist J, Gladden W K *Phys. Rev. B* **27** 4833 (1983)
35. Esaev D G, Sinitsa S *Sov. Tech. Phys. Lett.* **14** 440 (1986); *Pis'ma Zh. Tekh. Fiz.* **12** 1063 (1986)
36. Esaev D G, Sinitsa S P *Microelectron. Eng.* **22** 211 (1993)
37. DiMaria D J et al. *Phys. Rev. Lett.* **57** 3213 (1986)
38. Fischetti M V et al. *Phys. Rev. B* **35** 4404 (1987)
39. Sorokin A N, Karpushin A A, Gritsenko V A, Wong H *J. Appl. Phys.* **105** 073706 (2009)
40. Nekrashevich S S, Gritsenko V A *J. Appl. Phys.* **110** 114103 (2011)
41. Gritsenko V A, Perevalov T V *Fizika Dielektricheskikh Plenok: Atomnaya i Elektronnaya Struktura* (Physics of Dielectric Films: Atomic and Electronic Structure) (Novosibirsk: Avtograf, 2015)
42. Nasyrov K A, Gritsenko V A et al. *J. Appl. Phys.* **96** 4293 (2004)
43. Nasyrov K A, Gritsenko V A *Phys. Usp.* **56** 999 (2013); *Usp. Fiz. Nauk* **183** 1099 (2013)
44. DiMaria D J, Abernathey J R *J. Appl. Phys.* **60** 1727 (1986)